Check for updates

How to cite: *Angew. Chem. Int. Ed.* **2020**, *59*, 20224–20229
International Edition: doi.org/10.1002/anie.202005883
German Edition: doi.org/10.1002/ange.202005883

Catalyst Activation **Hot Paper**

On the Promotion of Catalytic Reactions by Surface Acoustic Waves

*Bernhard von Boehn, Michael Foerster, Moritz von Boehn, Jordi Prat, Ferran Macià, Blai Casals, Muhammad Waqas Khaliq, Alberto Hernández-Mínguez, Lucia Aballe, and Ronald Imbihl**

Abstract: *Surface acoustic waves (SAW) allow to manipulate surfaces with potential applications in catalysis, sensor and nanotechnology. SAWs were shown to cause a strong increase in catalytic activity and selectivity in many oxidation and decomposition reactions on metallic and oxidic catalysts. However, the promotion mechanism has not been unambiguously identified. Using stroboscopic X-ray photoelectron spectro-microscopy, we were able to evidence a sub-nanosecond work function change during propagation of 500 MHz SAWs on a 9 nm thick platinum film. We quantify the work function change to 455 μeV. Such a small variation rules out that electronic effects due to elastic deformation (strain) play a major role in the SAW-induced promotion of catalysis. In a second set of experiments, SAW-induced intermixing of a five monolayers thick Rh film on top of polycrystalline platinum was demonstrated to be due to enhanced thermal diffusion caused by an increase of the surface temperature by about 75 K when SAWs were excited. Reversible surface structural changes are suggested to be a major cause for catalytic promotion.*

Introduction

In sonochemistry chemical reactions are initiated by acoustic waves, an effect successfully demonstrated both in the liquid phase and in solid state reactions.[1] In heterogeneous catalysis a strong promotion effect by bulk and surface acoustic waves has been shown for several oxidation and decomposition reactions on metal and metal oxide catalysts.[2,3] In a surface acoustic wave (SAW) periodic distortions of the surface with an amplitude of a few nm and a wavelength of several μm propagate across the surface with the velocity of sound in a solid, i. e., with about 4000 $m\,s^{-1}$ in the case of $LiNbO_3$.[4] The amplitude of SAWs decays exponentially in the bulk. In ethanol oxidation over palladium, copper or silver metal catalysts rate-increases by SAWs up to a factor of five have been found.[5] In UHV type experiments SAWs were found to increase the rate of catalytic CO oxidation over a Pt(110) single crystal by up to a factor of six.[6,7]

The promotion of catalytic reactions by SAWs is of interest, first of all, because a non-thermal activation of catalytic reactions might be favorable for the optimization of yield and selectivity. Secondly, the mechanistic understanding of the promotion effect represents a challenging scientific problem. Finally, a detailed mechanistic understanding of the processes occurring during the excitation and propagation of SAW might help to develop novel nano-patterning approaches that could be used for sensors and nanoscale design of surfaces.[8]

Soon after the discovery of the catalytic promotion effect by SAWs, studies with surface analytical techniques were started, aiming at elucidating the mechanism of the promotion effect.[3] Infrared absorption spectroscopy (IRAS) revealed that SAWs can induce a site change of CO adsorbed on copper surfaces.[9] On/off experiments with photoelectron emission microscopy (PEEM) demonstrated that SAWs cause reversible changes of the work function (WF) on the metal surfaces of copper, palladium and gold.[10] Based on these results, it was concluded, that the catalytic promotion effect is due to electronic effects induced by SAWs.[3] Strain is known to affect the reactivity of solid surfaces, but in order to cause significant changes in the activation barriers of surface processes, the lattice constant should change by at least 10^{-3}.[11] A SAW with a wavelength of 8 μm (500 MHz) and a high power density of 165 $W\,m^{-1}$, however, produces a maximum strain below 5×10^{-4}.

The catalytic promotion effect of SAWs poses a challenging problem for theory, since the frequency ν of SAWs is with 10^6–10^9 Hz about five to eight orders of magnitude below the frequency required for energy quanta, $h\nu$, to have an activating effect on surface processes. However, molecular dynamics (MD) and kinetic Monte Carlo simulations predicted that SAWs can enhance surface diffusion by a factor of 4.5×10^3.[12,13] Besides an adiabatic temperature rise and strain caused by SAWs, the enhancement was attributed to the coupling of high frequency harmonics generated due to the

[*] B. von Boehn, M. von Boehn, Prof. Dr. R. Imbihl
Institut für Physikalische Chemie und Elektrochemie,
Leibniz Universität Hannover
30167 Hannover (Germany)
E-mail: imbihl@pci.uni-hannover.de
Dr. M. Foerster, J. Prat, M. W. Khaliq, Dr. L. Aballe
ALBA Synchrotron Light Source
08290 Cerdanyola del Valles (Spain)
Dr. F. Macià
Dept. of Condensed Matter Physics, University of Barcelona
08028 Barcelona (Spain)
Dr. B. Casals
Institut de Ciència de Materials de Barcelona (ICMAB-CSIC)
08193 Bellaterra (Spain)
Dr. A. Hernández-Mínguez
Paul-Drude-Institut für Festkörperelektronik,
Leibniz-Institut im Forschungsverbund Berlin e.V.
10117 Berlin (Germany)
Supporting information and the ORCID identification number(s) for the author(s) of this article can be found under: https://doi.org/10.1002/anie.202005883.

© 2020 The Authors. Published by Wiley-VCH GmbH. This is an open access article under the terms of the Creative Commons Attribution Non-Commercial License, which permits use, distribution and reproduction in any medium, provided the original work is properly cited, and is not used for commercial purposes.

nonlinear sharpening of SAWs to vibrational modes of the adsorbates. Experimentally, a smaller enhancement of the surface diffusion coefficient of Au clusters on a Si(111) surface by a factor of 19 was found.[13] Similarly, in a MD simulation the non-linear properties of SAWs were made responsible for the promotion of catalytic CO oxidation on a (110) oriented Pt surface.[14] The promotion effect was attributed to shock spikes caused by SAWs, which would enhance the diffusion and desorption of adsorbed CO molecules.

None of the above cited explanations can explain the time scale with which the reaction rate responds to SAWs. Electronic effects should cause an immediate response of the catalytic surface, but experimentally the rate responds with a delay of several tens of seconds to minutes.[3] This delayed response is also observed in UHV-type experiments on Pt(110), where transport limitations play no role. This unsolved question was the primary motivation for us to look into the mechanism of catalytic promotion by SAWs in a systematic manner. Besides an electronic effect, SAW might also induce changes in the arrangement of surface atoms, i. e. cause surface restructuring, which could enhance the catalytic activity. We assess the electronic effects by taking advantage of the time structure of synchrotron radiation that allows us to take stroboscopic photoelectron emission images of the waves with a time resolution below 100 ps,[15] and thus detect changes in the local WF as a function of the SAW phase. For the detection of restructuring effects, we designed a bimetallic model catalyst with a vertically layered structure that enables measuring vertical intermixing induced by SAWs. Our results allow ruling out one of the proposed promotion mechanisms for SAWs and provide a physical basis for further research on possible promotion mechanisms.

Results

In order to measure the influence of SAW on the local work function and on the surface composition, we perform two different types of experiments. The experimental set-ups are sketched in Figure 1 a. In both cases, $LiNbO_3$ crystals equipped with interdigital transducer electrodes (IDTs) serve as substrate and source for SAWs. SAWs are excited by feeding an AC signal in the MHz range to the IDTs. For measuring SAW-induced work function changes, a micro-structured Pt film of 20 nm thickness (reduced to roughly 9 nm during surface cleaning before the experiments) is deposited on top of the $LiNbO_3$ crystal. A photo of the Pt/$LiNbO_3$ sample surface is shown in Figure 1 b. For probing the effect of SAWs on the surface composition, an ordered array of five monolayers thick, square Rh patches (approximately $50 \times 50\ \mu m^2$ size each square) is deposited in situ onto the Pt stripe, as can be seen in the LEEM image in Figure 1 c. In this way, laterally resolved X-ray photoemission spectra can be recorded simultaneously on Rh-covered and uncovered parts of the Pt stripe. A schematic plot showing regions of compressive and tensile strain during propagation of a SAW is depicted in Figure 1 d.

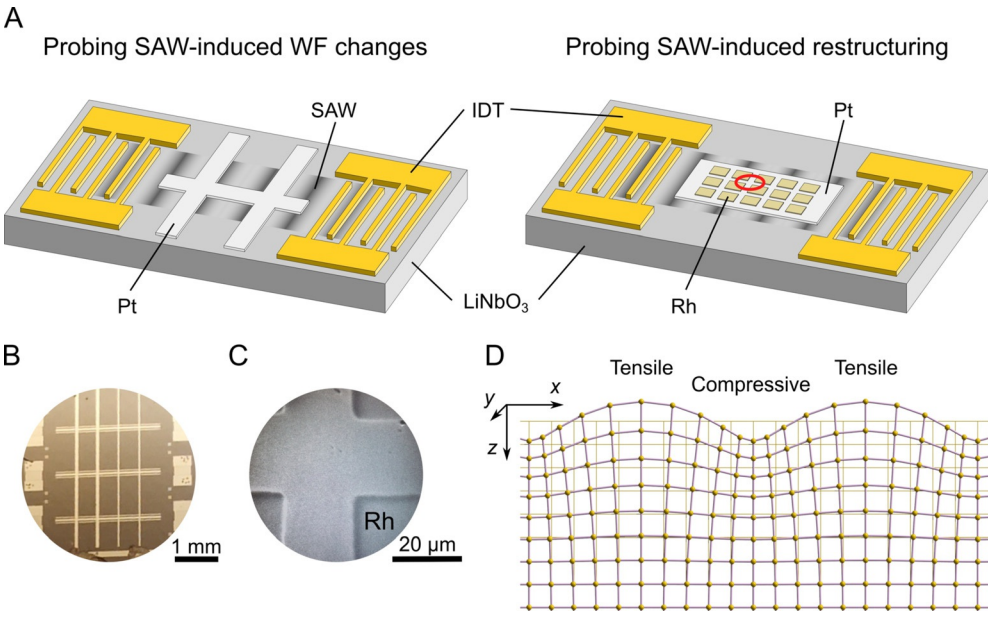

Figure 1. Experimental set-up for the excitation of SAWs on microstructured metal films on top of a piezoelectric material. a) $LiNbO_3$ single crystals with IDTs and metal films. Left: Schematic view of a micro-structured Pt film used for detection of SAW-induced WF changes. Right: Schematic view of a micro-structured Pt/Rh film constructed for the detection of SAW-induced intermixing of the metallic constituents; Pt film thickness: ≈9 nm (left) and ≈40 nm (right), Rh film thickness: ≈5 ML (right). b) Photography of the micro-structured Pt film. c) LEEM image of the microstructured Pt/Rh film. The area corresponding to the LEEM image is highlighted by a red circle in a. d) Schematic plot showing regions of compressive and tensile strain during propagation of a SAW.

© 2020 The Authors. Published by Wiley-VCH GmbH

15213773, 2020, 45, Downloaded from https://onlinelibrary.wiley.com/doi/10.1002/anie.202005883 by Technische Informationsbibliothek, Wiley Online Library on [16/10/2023]. See the Terms and Conditions (https://onlinelibrary.wiley.com/terms-and-conditions) on Wiley Online Library for rules of use; OA articles are governed by the applicable Creative Commons License

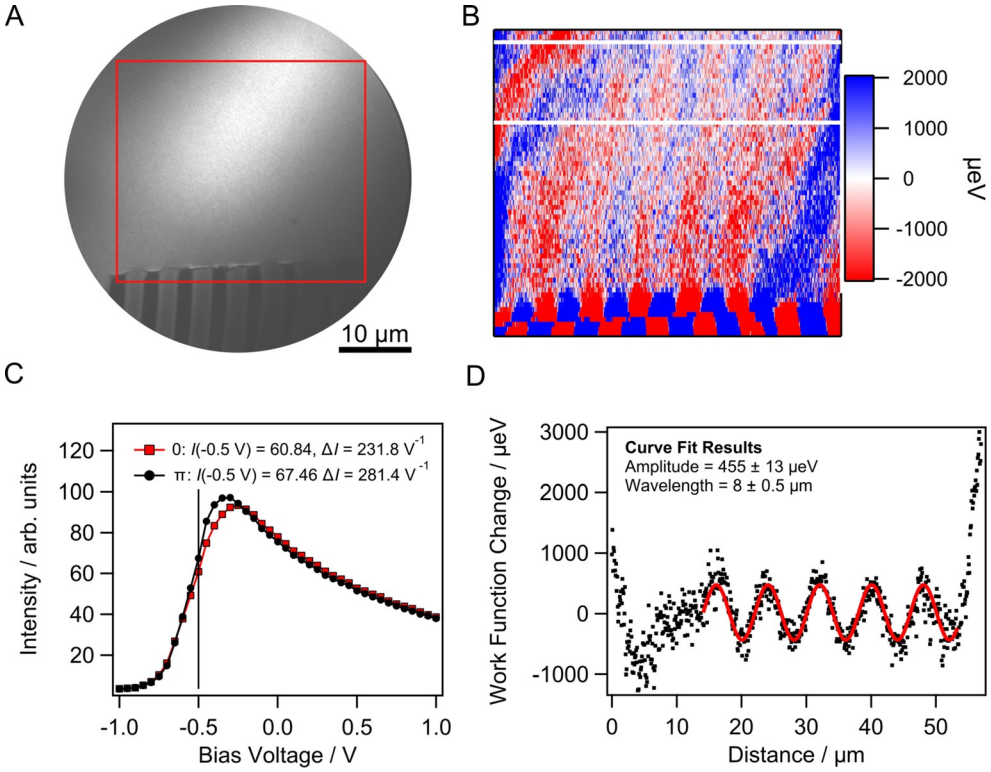

Figure 2. Determination of the local WF change during propagation of a ≈500 MHz SAW on a Pt film at 300 K. a) Stroboscopic XPEEM image of a Pt domain (upper part) and the adjacent $LiNbO_3$ surface area (lower part) recorded with a photon energy of 300 eV at −0.5 eV bias voltage. In the raw data the SAW is visible only on the free $LiNbO_3$ surface where it causes a variation of the surface potential of 1.3 eV amplitude. The red frame marks the window used for subsequent data analysis. b) Differential image of two stroboscopic XPEEM images phase-shifted by $\Delta\phi = \pi$. The total integration time is 70 min for the image. c) Photoelectron spectra of a Pt domain around the cut-off energy as obtained from stroboscopic XPEEM image stacks for opposite SAW phases (0 and π). The vertical line marks the bias voltage at which the images in a and b were taken. d) Local WF change as function of the position in a propagating SAW, and numerical fit with a sine function. For this plot the data between the two white lines in b were averaged.

SAW-Induced Work Function Changes

The design of the IDTs on the $LiNbO_3$ crystal is tuned to generate SAWs with a wavelength of 8 µm at a frequency exactly matched to the repetition rate of the X-ray pulses generated by the ALBA Synchrotron in the multi-bunch mode (499.654 MHz). For determining the local WF, spectroscopic XPEEM images are taken with the electron kinetic energy close to zero, i. e. at the low energy photoelectron cut-off. As shown in Figure 2c, the photoelectron yield varies steeply at the chosen sample bias voltage of −0.5 eV and thus the local image brightness sensitively depends on shifts of the cut-off energy, i. e., on variations of the WF.

On the free $LiNbO_3$ surface the SAWs are readily visible in PEEM because, being an insulating piezoelectric material, the acoustic waves are accompanied by a variation of the surface potential of up to 3 V amplitude.[15] Collecting stroboscopic images with 2 ns separation, the propagating SAWs are directly imaged on the uncovered $LiNbO_3$, as shown at the bottom of Figure 2a. For a single stroboscopic image, long integration times can be used because between two synchrotron light pulses, the synchronized SAW advances by exactly one wavelength, overlaying multiple identical partial images on the detector. In contrast, on the Pt film, the variations in the $LiNbO_3$ surface potential are completely shielded by the equipotential metal surface (for details on the electrical characterization and film morphology please refer to the supplementary information).

In order to highlight small brightness variations caused by local WF changes induced by SAWs, expected to be at most in the meV range, two stroboscopic images with opposite SAW phase (i. e., shifted by π) were recorded for every measurement. By subtracting the two phase-shifted images, each integrated over 35 min, all other inhomogeneities cancel out, whereas only the amplitude of brightness variations caused by SAWs should double. An example of one of the two recorded phases is shown in Figure 2a, and the result of such an image subtraction in Figure 2b.

From the slope of the spectra in Figure 2c, the XPEEM intensity variations in Figure 2b can be converted into local WF changes (please refer to the supplementary information for details). The results are displayed in Figure 2d. An intensity cross section averaged over the area highlighted by the two vertical lines in Figure 2b, reveals a variation of the local WF with an 8 µm periodicity, equal to the SAW wavelength. The SAWs thus clearly cause a local change of the WF, but the amplitude of these WF changes is with 455 ± 13 µeV very small (± 13 µeV representing the statistical

 © 2020 The Authors. Published by Wiley-VCH GmbH

15213773, 2020, 45, Downloaded from https://onlinelibrary.wiley.com/doi/10.1002/anie.202005883 by Technische Informationsbibliothek, Wiley Online Library on [16/10/2023]. See the Terms and Conditions (https://onlinelibrary.wiley.com/terms-and-conditions) on Wiley Online Library for rules of use; OA articles are governed by the applicable Creative Commons License

error). In order to make sure that the dependence shown in Figure 2c is not an artifact due to an electrostatic effect caused by potential variations in the adjacent area of Pt-free $LiNbO_3$, line scans were taken at varying distances from the domain boundary (please refer to the supplementary information). In fact, a strong intensity variation with the SAW periodicity is seen at the border of the Pt stripe. The phase of this intensity variation is, however, shifted by approximately π with respect to the SAW as visible on the $LiNbO_3$ crystal, and its intensity decreases fast with increasing distance from the stripe border, until finally only a very weak intensity variation is visible in phase with the SAW on $LiNbO_3$, which is the true signal of the WF modulation.

The zero in the plot of Figure 2d represents areas of zero intensity in the difference image, and thus no WF difference. Compressive and tensile strain of the SAWs should cause asymmetric changes in the WF, as the effect on electron density is opposite. DFT calculations conducted for a Pt(100) surface demonstrated that compressive strain increases the WF while tensile strain decreases it.[16] Since the essential parameter is the change in the electron density, one can estimate the WF change from the relative volume change. Using the linear relation given in ref. [16] one arrives at a theoretical estimate of approximately 13.4 meV per 1% volume change. In our experiment the strain, and thus the relative volume change, can be computed easily (please refer to the supplementary information for details). From the SAW surface potential amplitude of 1.3 V we calculate a volume change of 1.6×10^{-4}, which translates to an estimated 28.4 meV work function change per 1% volume change, in reasonable agreement with the theoretical estimate. We note here that, since the relative volume change caused by SAWs depends on the material, the SAW-induced work function variations might be substantially larger on a softer material.

The WF changes caused by SAWs of less than 1 meV are very small in comparison to those caused by adsorbates or surface restructuring, mostly in the range 0.1–1 eV, and in the case of alkali adsorbates even above 1 eV.[17] The small WF changes caused by SAWs rule out that strain induced electronic effects play a significant role in the promotion of catalysis by SAWs. However, in on/off experiments Inoue et al. found WF changes induced by SAWs on copper, gold and palladium surfaces.[10] These WF changes were not completely reversible—only to about 60–70%—and had an associated time constant of several tens of seconds. The PEEM intensity had not been calibrated, but since PEEM is able to detect WF changes ≥ 1 meV,[18] one can estimate that Inoue et al. observed WF changes of at least a few meV. If these were the result of changes in the electronic structure, they should *i)* appear instantly, and *ii)* disappear as soon as SAWs are turned off. We also found a permanent WF decrease of 30 to 75 meV in the Pt areas exposed to SAW for several hours with respect to Pt areas not exposed to SAW. However, we attribute such decrease to changes in the surface structure due to prolonged exposure to SAWs (for details please refer to the supplementary information).

SAW-Induced Structural Changes

The question on the nature of the reversible and slow WF changes caused by SAWs finds a convincing answer if one takes into account the possibility of induced structural changes. Surface roughening is associated with a WF decrease, a phenomenon known as the Smoluchowski effect.[19] The creation of structural surface defects like vacancies, atomic steps or of structural disorder is a slow process and since surface roughening in general is known to increase the reactivity of surfaces, the catalytic promotion effect of SAWs may find a simple answer. Severe morphological changes, including destructions visible by eye, were found on the Pt(110) single crystal exposed to SAW.[20] However, the authors concluded that these dramatic effects, which by nature were irreversible, were not responsible for the main part of the promotion of catalytic CO oxidation by SAWs.

In order to detect restructuring effects, a model system is created by depositing a few atomic layers thick (≈ 5 layers) Rh film on top of a 40 nm Pt stripe. As shown in Figure 1a (right side), a micro-structured design is used, in which an uncovered part of the Pt film serves as reference to monitor the degree of Rh/Pt intermixing. If the SAWs promote diffusion in the vertical direction, then we should observe a change in the microspot-XPS ratio of the Pt signal between an area covered with a Rh patch and the surrounding uncovered area. Just for entropic reasons the two metals should mix but also enthalpy provides a driving force for segregation and therefore intermixing, since the surface energy of Pt is lower than that of Rh.[21]

Exposing the surface at 300 K to SAWs of varying frequency (125, 250, and 500 MHz) and power (up to approximately 1 W) for periods ranging from one to several hours did not cause any detectable changes in the surface composition. Only when we raise the nominal sample temperature to 400 K and switch on SAWs at 125 MHz (the frequency at which the maximum power arrives at the sample) we observe intermixing. Switching on the SAWs causes a temperature rise to 445 K, as measured with a thermocouple attached to a supporting Ta sheet below the $LiNbO_3$ substrate. In these conditions over a period of 13 hours, the Pt 4f signal normalized to the signal of the free Pt surface increases by a factor of ≈ 1.75, as shown in Figure 3a.

The expected Pt enrichment in the surface is found, but the question is whether the effect can be explained by thermally activated diffusion alone. Therefore, we prepared a $LiNbO_3$ sample completely covered by 40 nm Pt with a three monolayers thick Rh film on top, and followed the changes in composition during heating up by means of Auger electron spectroscopy (AES). The results displayed in Figure 3b show that Pt segregation to the surface starts to become significant at ≈ 475 K, which is only 30 K above the 445 K measured below the substrate bottom phase during the SAW experiment. In fact, measuring the sample surface temperature directly with a pyrometer during SAW application showed that the temperature measured by the thermocouple below the substrate underestimates the SAW induced heating of the surface by up to 30 K. Thus the Rh/Pt

 © 2020 The Authors. Published by Wiley-VCH GmbH

15213773, 2020, 45, Downloaded from https://onlinelibrary.wiley.com/doi/10.1002/anie.202005883 by Technische Informationsbibliothek, Wiley Online Library on [16/10/2023]. See the Terms and Conditions (https://onlinelibrary.wiley.com/terms-and-conditions) on Wiley Online Library for rules of use; OA articles are governed by the applicable Creative Commons License

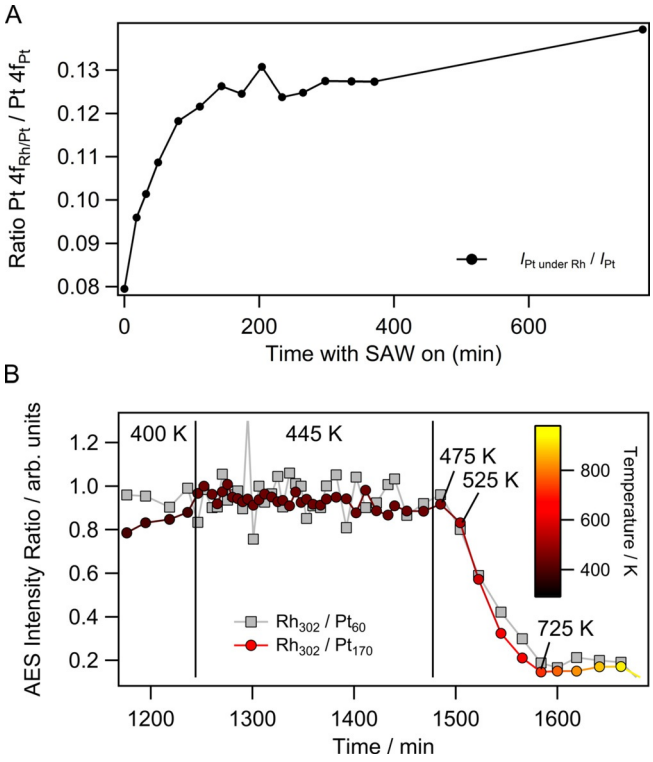

Figure 3. SAW-induced and thermally-induced intermixing in a layered Rh/Pt surface. a) SAW-induced Pt enrichment as a function of SAW application time (125 MHz, ≈0.1 W, 445 K substrate temperature). A Pt/Rh microstructure consisting of a 5 ML thick Rh film on top of a 40 nm Pt film as displayed in Figure 1c is used. Shown is the Pt 4f intensity of Rh covered Pt area normalized with respect to the Pt 4f intensity of the uncovered Pt area. b) Thermally induced Pt enrichment on the surface of 3 ML thick Rh film on top of ≈40 nm Pt on $LiNbO_3$. The Rh/Pt Auger intensity ratio is followed while slowly heating up. Intermixing starts above about 475 K, as reflected by a steep decrease of the Rh/Pt signal.

intermixing seen in Figure 3a can be explained by thermal diffusion alone.

Discussion

In previous experiments with a 500 nm thick Pt(110) single crystal a temperature increase due to SAWs of 30–50 K was found, in agreement with our results.[7] This temperature rise will contribute to the promotion effect, but Mitrelias et al. clearly demonstrated that it alone could not explain the increase of catalytic CO oxidation by SAWs. Based on the finding that SAWs reversibly reduce the WF of a Pt(110) crystal held in pure CO, it was concluded that SAWs induce the desorption of CO.[6] The removal of CO from a CO-adlayer inhibiting O_2-adsorption could certainly explain an activation of the CO + O_2 reaction by SAWs, but the experimentally observed time constant of several tens of seconds does not agree with such a conclusion. On the other hand, a SAW-induced roughening of the Pt(110) surface would also lead to activation and could explain the long time constants associated with activation. This latter explanation needs, however, to be reconciled with the above result that SAWs leave the surface essentially intact.[22]

The finding by Inoue et al. that SAWs cause slow reversible WF changes of metal surfaces held in vacuum strongly suggests that reversible structural changes of the surface take place and that these changes contribute to the catalytic enhancement by SAWs. If the SAWs generate unstable non-equilibrium configurations of the surface atoms, then, after switching off the SAWs, the surface atoms would return to their equilibrium configurations, explaining the long time constants observed in on/off experiments. This explanation is compatible with our segregation experiment, since only small structural changes can be involved if the process is to be reversible. Molecular dynamics simulation that are currently in progress in fact demonstrate that shock fronts which arise due to a nonlinear sharpening of SAWs can cause structural modifications of the surface.[23] The theoretical results could be further substantiated by scanning tunneling microscopy (STM) measurements, for example, before and after exposing a thin Pt crystal to strong SAW ex-citation.

We briefly review the possible factors contributing to a promotion of catalytic reaction by SAWs:

(i) Changes in the electronic structure
(ii) Elastic strain modifying energy barriers
(iii) Dynamic coupling effects of vibrational modes with nonlinear components of SAWs
(iv) Temperature rise due to energy dissipation of SAWs
(v) Adiabatic temperature changes
(vi) Structural changes

We can rule out electronic effects as significant factor on the basis of our results. Similarly, the elastic strain caused by SAW is estimated to be with less than 5×10^{-4} too small to substantially reduce energy barriers. In contrast, the dynamic coupling of vibrational modes of the surface with nonlinear components of SAWs as well as the temperature increase resulting from dissipated energy of the SAWs may very well contribute to the promotion effect.[12] In addition, we have to consider the adiabatic temperature variations caused by an expansion/contraction of the surface region during propagation of SAWs. Simulations demonstrated that their amplitude can reach 5% of the average temperature. Since positive and negative temperature variations do not cancel out in Arrhenius law, this effect can significantly enhance a catalytic rate.[12] Finally, a number of indirect evidences strongly suggest that reversible surface restructuring caused by SAWs plays an important role, in particular, in explaining the long time constants that are often observed. Effects that rely on the nonlinear components of SAWs such as dynamic coupling and SAW-induced restructuring are expected to strongly depend on the SAW amplitude and on the surface structure. Further experiments are needed to fully quantify each of the remaining possible contributions.

Conclusion

In summary, in order to disentangle different contributions we have studied elementary surface processes that can

© 2020 The Authors. Published by Wiley-VCH GmbH

15213773, 2020, 45, Downloaded from https://onlinelibrary.wiley.com/doi/10.1002/anie.202005883 by Technische Informationsbibliothek, Wiley Online Library on [16/10/2023]. See the Terms and Conditions (https://onlinelibrary.wiley.com/terms-and-conditions) on Wiley Online Library for rules of use; OA articles are governed by the applicable Creative Commons License

underlie a promotion of catalytic reactions by SAWs. Using stroboscopic imaging, we demonstrated that SAWs cause a work function change in the range of hundreds of μeV on a polycrystalline Pt film. Such small changes rule out electronic effects as cause for SAW enhancement of catalytic surface reactions. Using a layered bimetallic Rh/Pt film we showed that SAWs leave the surface structure essentially intact, i. e., they usually do not lead to irreversible structural changes. The catalytic promotion effect by SAWs results from a combination of several factors. A major role we can attribute to the increase in the average surface temperature by as much as 75 K, to which we have to add periodic temperature changes caused by adiabatic expansion/contraction of the surface during SAWs. Moreover, we expect dynamic coupling of vibrational surface modes with higher harmonics resulting from nonlinear sharpening of SAWs to contribute. We hope our work triggers other quantitative studies in order to finally arrive at a detailed understanding of the mechanisms underlying the promising effect of catalytic promotion by surface acoustic waves.

Acknowledgements

The authors thank Werner Seidel for technical support in the fabrication of the IDTs, Rolf J. Haug, Hannover, for help in preparation of the samples, and Leo Zhigilei for carefully reading the manuscript. The research leading to this result has been supported by the project CALIPSOplus under Grant Agreement 730872 from the EU Framework Programme for Research and Innovation HORIZON 2020. LA and MF acknowledge support from Spanish MINECO through Grant No. RTI2018-095303-B-C53. FM and BC acknowledges support from Spanish MINECO through Grants No. RYC-2014-16515, No. MAT2015-69144-P, No. SEV-2015-0496 and No. MAT2017-85232-R. Open access funding enabled and organized by Projekt DEAL.

Conflict of interest

The authors declare no conflict of interest.

Keywords: heterogeneous catalysis · LEEM · PEEM · Surface acoustic waves · work function

[1] T. J. Mason, J. P. Lorimer, *Sonochemistry. Theory, applications and uses of ultrasound in chemistry*, Wiley, New York, **1988**.
[2] Y. Inoue, *MRS Bull.* **2019**, *44*, 361.
[3] Y. Inoue, *Surf. Sci. Rep.* **2007**, *62*, 305.
[4] a) B. A. Auld, *Acoustic fields and waves in solids*, Wiley, New York, **1973**; b) M. E. Lines, A. M. Glass, *Principles and Applications of Ferroelectrics and Related Materials*, Oxford University Press, Oxford, **2001**.
[5] Y. Inoue, Y. Watanabe, *Catal. Today* **1993**, *16*, 487.
[6] S. Kelling, S. Cerasari, H. H. Rotermund, G. Ertl, D. A. King, *Chem. Phys. Lett.* **1998**, *293*, 325.
[7] T. Mitrelias, S. Kelling, R. I. Kvon, V. P. Ostanin, D. A. King, *Surf. Sci.* **1998**, *417*, 97.
[8] a) S. Okuda, T. Ono, Y. Kanai, T. Ikuta, M. Shimatani, S. Ogawa, K. Maehashi, K. Inoue, K. Matsumoto, *ACS Sens.* **2018**, *3*, 200; b) Z. Ma, J. Guo, Y. J. Liu, Y. Ai, *Nanoscale* **2015**, *7*, 14047; c) J. B. Kinzel, D. Rudolph, M. Bichler, G. Abstreiter, J. J. Finley, G. Koblmüller, A. Wixforth, H. J. Krenner, *Nano Lett.* **2011**, *11*, 1512; d) D. J. Collins, B. Morahan, J. Garcia-Bustos, C. Doerig, M. Plebanski, A. Neild, *Nat. Commun.* **2015**, *6*, 8686; e) C. Taillan, N. Combe, J. Morillo, *Phys. Rev. Lett.* **2011**, *106*, 76102; f) B. Paschke, A. Wixforth, D. Denysenko, D. Volkmer, *ACS Sens.* **2017**, *2*, 740.
[9] a) H. Nishiyama, Y. Inoue, *Surf. Sci.* **2005**, *594*, 156; b) H. Nishiyama, Y. Inoue, *J. Phys. Chem. B* **2003**, *107*, 8738.
[10] H. Nishiyama, Y. Inoue, *Surf. Sci.* **2006**, *600*, 2644.
[11] a) M. Mavrikakis, B. Hammer, J. K. Nørskov, *Phys. Rev. Lett.* **1998**, *81*, 2819; b) D. J. Shu, F. Liu, X. G. Gong, *Phys. Rev. B* **2001**, *64*, 441.
[12] C. Wu, V. Y. Zaitsev, L. V. Zhigilei, *J. Phys. Chem. C* **2013**, *117*, 9252.
[13] M. V. Shugaev, A. J. Manzo, C. Wu, V. Y. Zaitsev, H. Helvajian, L. V. Zhigilei, *Phys. Rev. B* **2015**, *91*, 8.
[14] Q. An, J. Qian, R. R. Nielsen, L. Sementa, G. Barcaro, F. R. Negreiros, A. Fortunelli, W. A. Goddard III, *J. Mater. Chem. A* **2016**, *4*, 12036.
[15] M. Foerster, N. Statuto, B. Casals, A. Hernández-Mínguez, S. Finizio, A. Mandziak, L. Aballe, J. M. Hernàndez Ferràs, F. Macià, *J. Synchrotron Radiat.* **2019**, *26*, 184.
[16] X. F. Wang, L. He, S. Halas, T. Pieńkos, J. G. Lin, T. Durakiewicz, *Appl. Phys. Lett.* **2013**, *102*, 223504.
[17] P. S. Bagus, D. Käfer, G. Witte, C. Wöll, *Phys. Rev. Lett.* **2008**, *100*, 126101.
[18] H. H. Rotermund, *Surf. Sci. Rep.* **1997**, *29*, 265.
[19] R. Smoluchowski, *Phys. Rev.* **1941**, *60*, 661.
[20] S. Kelling, N. Saito, Y. Inoue, D. A. King, *Appl. Surf. Sci.* **1999**, *150*, 47.
[21] A. Christensen, A. V. Ruban, P. Stoltze, K. W. Jacobsen, H. L. Skriver, J. K. Nørskov, F. Besenbacher, *Phys. Rev. B* **1997**, *56*, 5822.
[22] S. Ladas, R. Imbihl, G. Ertl, *Surf. Sci.* **1988**, *197*, 153.
[23] M. V. Shugaev, C. Wu, V. . Y. Zaitsev, L. V. Zhigilei, *J. Appl. Phys.* **2020**, *128*, 045117.

Manuscript received: April 23, 2020
Revised manuscript received: July 8, 2020
Accepted manuscript online: July 30, 2020
Version of record online: September 9, 2020

 © 2020 The Authors. Published by Wiley-VCH GmbH

15213773, 2020, 45, Downloaded from https://onlinelibrary.wiley.com/doi/10.1002/anie.202005883 by Technische Informationsbibliothek, Wiley Online Library on [16/10/2023]. See the Terms and Conditions (https://onlinelibrary.wiley.com/terms-and-conditions) on Wiley Online Library for rules of use; OA articles are governed by the applicable Creative Commons License